

ORIGINAL ARTICLE

The Energy-absorbing Characteristics of Single Spherical-roof Contoured-core (SRCC) Cell with Composite Materials

Quanjin Ma^{1,2*}, M.R.M. Rejab^{1,2}, Shaofu Kang², M.S. Idris¹ and M.A.A.M. Zin¹¹Structural Performance Materials Engineering (SUPREME) Focus Group, Faculty of Mechanical and Automotive Engineering Technology, Universiti Malaysia Pahang, 26600 Pekan, Pahang, Malaysia

Phone: +60172667860

²School of Mechanical Engineering, Ningxia University, 750021 Yinchuan, China

ABSTRACT – It is a challenging task to manufacture the novel lightweight sandwich panel with different composite materials. The aim of this paper is to study the energy-absorbing characteristics of single spherical-roof contoured-core cell with carbon, glass and aramid fibre reinforced plastics, which were fabricated through compression moulding technique. The quasi-static compression test was carried out to investigate the compressive properties and crushing behaviour of the single contoured-core cell. It was demonstrated that the single spherical-roof contoured-core with aramid fibre reinforced plastic provided the highest specific energy absorption value of 0.69 kJ and the lowest compressive stiffness of 30.43 kN/mm compared to carbon and glass fibre reinforced plastics. Furthermore, it was observed that matrix cracks, fibre fracture and laminate bending are the main failure modes of the single contoured-core cell under quasi-static loading.

ARTICLE HISTORYReceived: 25th Mar 2020Revised: 9th Oct 2020Accepted: 1st Dec 2020**KEYWORDS**

Energy-absorbing characteristics;
Spherical-roof;
Contoured-core;
Sandwich panel;
Quasi-static loading

INTRODUCTION

Nowadays, composite materials have been commonly used in many application areas such as aerospace, automotive, military and defence, and civil engineering [1-6], which depends on its superior stiffness, strength properties and higher flexural strength. Sandwich panel consists of two thin fibre reinforced plastics skins and the lightweight core structure. There are lots of investigations on the material types and core designs under different loading conditions [7-11]. It is known that various core structures have been proposed and studied in order to improve overall mechanical properties subjected to quasi-static and dynamic loading conditions, such as honeycomb cores [12-14], contoured cores [15], egg-box cores [16, 17], corrugated cores [18,19], foams [20, 21] and lattice cores [22, 23].

As a typical lightweight sandwich structure, a number of studies have been undertaken to investigate the mechanical properties of the sandwich panel with more elaborate core designs. For example, Sun et al. [12] investigated periodical grids to reinforced honeycomb core of sandwich structures, which indicated sandwich structure with grid-reinforced honeycomb could provide advanced structural properties. Rejab et al. [24] studied a series of experimental investigation and numerical analysis on the corrugated-core sandwich panel under compressive response, which provided a higher strength-to-weight ratio. Recently, composite contoured-core sandwich panels were designed and explored by Haldar et al. [15], which provided the superior compressive property compared to other core designs. In addition, the egg-box core sandwich panels have been manufactured using compression moulding technique, which offers higher compression strength at dynamic loading than quasi-static loading [16]. In order to provide higher stiffness and strength-to-weight ratio, polymethacrylimide (PMI) foam is used to fill in sandwich panels subjected to quasi-static and dynamic responses [25]. It was indicated that core density had a significant effect on the compressive strength of the sandwich panel. Furthermore, lattice truss core design is attracted much attention in many researchers, which includes octet-truss lattice core [26], pyramidal truss core [27-29], and 3D lattice truss core [30, 31].

Typically, two types of composite prepreg materials are used to manufacture composite sandwich panels, which refers to carbon fibre reinforced plastic (CFRP) and glass fibre reinforced plastic (GFRP). There have been many studies in recent years to develop the novel core designs [24, 32-34]. For example, Haldar et al. [15] summarised the variation of the quasi-static compressive response with core density made of CFRP and GFRP materials. It was known that as core density increased, CFRP material provided the superior properties compared to GFRP material. Meanwhile, Haldar et al. investigated on corrugated design based 3D printed sandwich panels subjected to quasi-static compression [35]. It was found that the increase in the contact area between the core and skins contributed to better mechanical properties. Quanjin et al. [36] studied the compressive properties on the spherical-roof contoured-core cell with different amounts of diamond-shaped notches. It was concluded that with the number of diamond-shaped notches increasing, compressive strength and modulus generally showed the decreasing trend. Although several works have been explored to develop core design and material type on the sandwich structure [37-39], there are limited studies on contoured-core design and aramid fibre reinforced plastic used as the potential lightweight sandwich panel. From the latest studies [15, 16], the contoured-core

sandwich panel provided the excellent energy-absorbing characteristics compared to other existed core designs. Therefore, it is a significant and meaningful study on this novel core with spherical-roof dome design.

This paper investigates the energy-absorbing characteristics of single spherical-roof contoured-core (SRCC) cell under quasi-static compressive loading. The single-cell specimens were made from three types of materials: carbon fibre/epoxy, glass fibre/epoxy and aramid fibre/epoxy. Specimens were manufactured using the compression moulding technique with contoured-core aluminium moulds. Moreover, compressive stiffness, peak load (F_{peak}), energy absorption (EA), specific energy absorption (SEA), and crushing behaviour are involved in this study.

MATERIALS AND METHODS

Materials Preparation

The resin system used was EpoxAmite™ 100 epoxy laminating system with 102 Hardener, supplied by Smooth-on, Inc, USA, which was mixed based on a recommended weight ratio of 100:29 [6]. It is a liquid type epoxy system used for various commercial applications, which relies on its unfilled, exceptional physical and better performance properties after curing process. Table 1 briefly provides the typical properties of the applied epoxy resin system. Three types of fabric sheets were supplied by Wuxi Weppom Composite Materials Co., China, which refers to carbon, glass and aramid fabric sheets. Table 2 summarises the physical specification of three types of fabric sheets.

Table 1. Typical properties of EpoxAmite™ 100 epoxy laminating system.

Specifications	EpoxAmite™ 100 Resin with 102 Medium Hardener
Mix ratio by volume	3:1
Mix ratio by weight	100:29
Mixed viscosity (Pa*s)	0.65
Pot life (Hour)	0.37
Cure time (Hour)	10-15
Specific gravity (kg/l)	1.11
Compressive strength (MPa)	75
Tensile elongation	3.15

Table 2. Specifications of carbon fibre, glass fibre and aramid fibre sheets.

Specifications		Carbon fibre	Glass fibre	Aramid fibre
		Carbon type	Glass type	Aramid type
Fibre material type		Carbon type	Glass type	Aramid type
Yarn count		3K	6K	3K
Weave pattern		Twill	Plain	Plain
Reinforcement yarn	Warp pattern	3K	6K	3K
	Weft pattern	3K	6K	3K
Fibre count (10 mm)	End count	5	2.2	n/a
	Pick count	5	2.2	n/a
Size thickness (mm)		0.3	0.4	0.8
Fabric area weight (g/m ²)		200	251-277	220

Specimen Fabrication

Three types of composite laminates materials were prepared using hand layup technique and a compression moulding technique. The aluminium 6061 contoured-core moulds were fabricated using the CNC machine. The male and female moulds were sprayed using the mould release agent (Mold Max® 20) to simplify the removal process. Composite laminates were properly laid into the aluminium mould and compressed together by platens of the hot press machine equipment for 24 hours for curing process, as shown in Figure 1(a). Figure 1(b) presents the fabrication of multi-cell specimens.

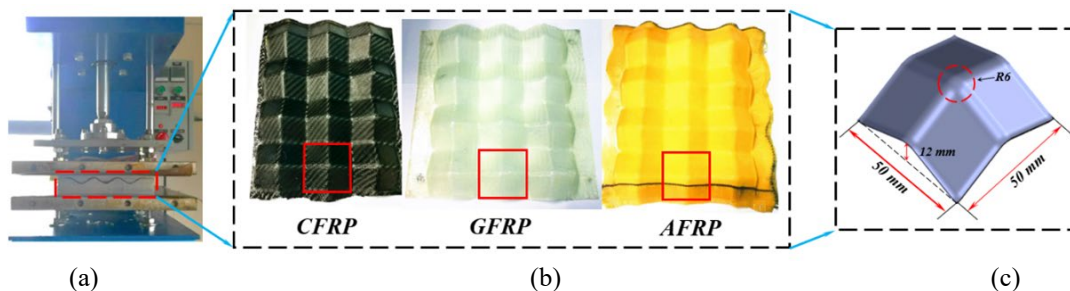


Figure 1. Fabrication procedure: (a) compression moulding technique; (b) initial samples; (c) the spherical-roof contoured-core structural dimension.

The single spherical-roof contoured-core (SRCC) cell was cut using a vertical cutting machine, and the structural dimension is presented in Figure 1(c). Figure 2 demonstrates the SRCC cell with CFRP, GFRP, aramid fibre reinforced plastic (AFRP) materials. The boundary edges of specimens were polished using a Forcipol 2V series grinding machine, which is a sufficient method to ensure the boundary condition and cutting quality of specimens.

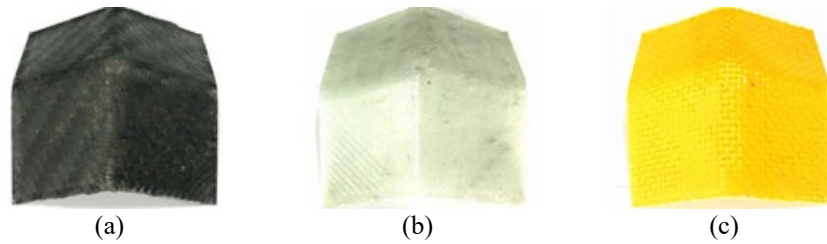


Figure 2. Images of (a) CFRP, (b) GFRP, and (c) AFRP single spherical-roof contoured-core cell.

Weight of the SRCC cell was measured using 8028-series professional digital scale with three decimal places, which provided accurate weight values. Table 3 summarises the several parameters of specimens in this study, which includes nominal thickness, nominal height, width, mass, and the number of plies. Three specimens were fabricated for each type of materials to two plies of carbon and glass fibre laminates, and one ply of aramid fibre laminate was used to manufacture around 1 mm thickness, respectively.

Table 3. Summary of single spherical-roof contoured-core cell specimens

Specimen ID	Nominal thickness (mm)	Nominal height (mm)	Width (mm)	Mass (g)	No. of plies
CFRP1	1	25	50	2.59	2
CFRP2	1	25	50	2.50	2
CFRP3	1	25	50	2.47	2
GFRP1	1	25	50	3.01	2
GFRP2	1	25	50	3.06	2
GFRP3	1	25	50	3.00	2
AFRP1	1	25	50	2.92	1
AFRP2	1	25	50	2.98	1
AFRP3	1	25	50	3.12	1

CFRP: carbon fibre reinforced plastic, GFRP: glass fibre reinforced plastic, AFRP: aramid fibre reinforced plastic

Experimental Procedure

The quasi-static compression loading tests used Instron 3369 model universal testing machine with a maximum load capability of 50 kN. The compression loading speed of the upper crosshead was set constant at 2 mm/minute, and specimens were unbonded condition under compression loading [36]. Specimens were crushed 80% of the initial height, and was used to study the crushing failure behaviour of a spherical-roof contoured-core cell. Crushing behaviour of the specimens with each 5 mm displacement was taken using a recorded camera during the quasi-static compression test. Figure 3(a) illustrated the schematic overview. The initial specimens with three types of materials were vertically put between two compressive platens with the unbonded condition, as shown in Figure 3(b).

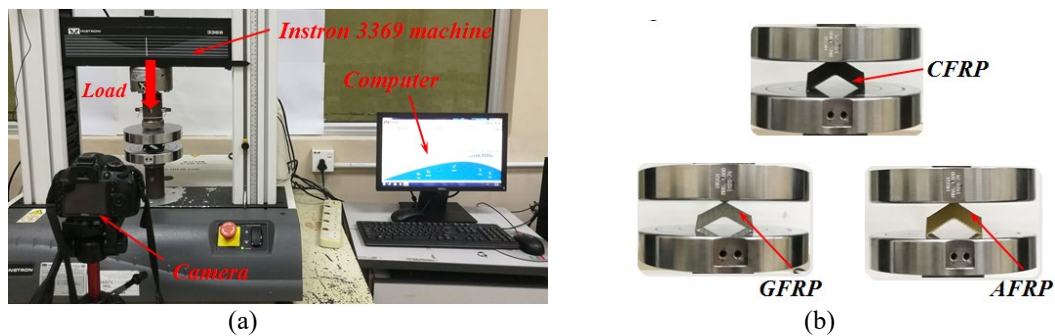


Figure 3. Experimental setup: (a) schematic overview; (b) quasi-static compression loading with three types of composite materials.

RESULTS AND DISCUSSION

Load versus displacement traces with three types of used composite materials are shown in Figure 4. CFRP and GFRP specimens showed a similar trend in the elastic deformation stage as reached the first peak loading point, which agreed with similar studies [13-14][36]. There are elastic and plastic deformation stages during in crushing deformation stage. In the elastic deformation stage, the crushing loading gradually increased to the first peak load, such as 0.49 kN for CFRP

specimen, 0.78 kN for GFRP specimen, and 0.42 kN for AFRP specimen. In the plastic deformation stage, the crushing loading dropped abruptly and floated or densification. AFRP specimens generally revealed an increasing loading trend as it deformed in the plastic deformation stage. It was observed that the crushing loading dropped with a small value after the first peak loading point, and slightly increased as compression displacement increased.

Comparison analysis on load versus displacement traces with three types of composite materials is briefly exhibited in Figure 5. The load increased to its peak load value with a series of small oscillations around the first peak value, which obtained 0.47 kN for CFRP specimen, and 0.78 kN for GFRP specimen. It was attributed to the matrix cracks around the spherical roof and four supporting points. Interestingly, the AFRP specimen showed a rapid upward trend compared to CFRP and GFRP specimens, which reached the maximum load value of 1.1 kN at 20 mm displacement.

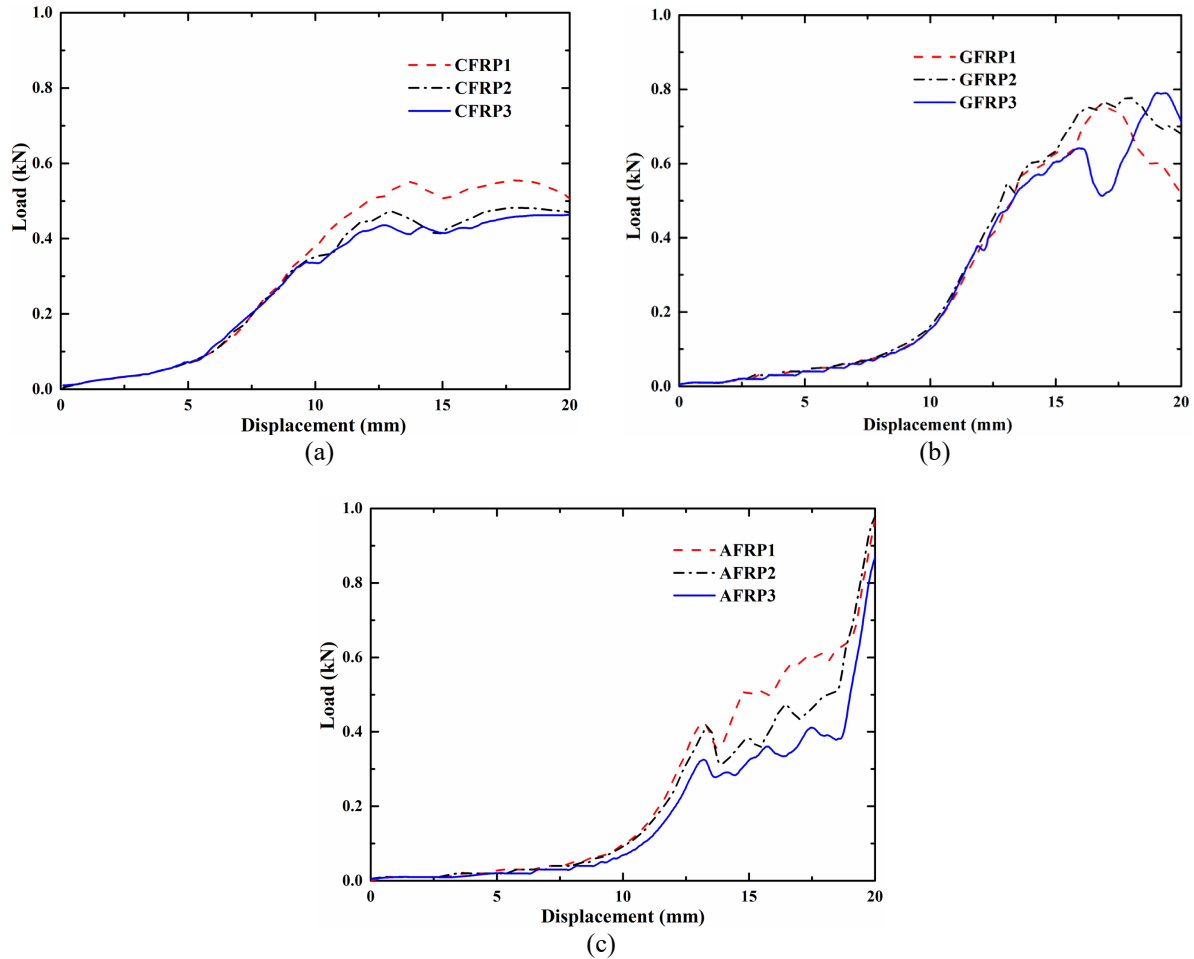


Figure 4. Graphs of load versus displacement traces in (a) CFRP, (b) GFRP and (c) AFRP.

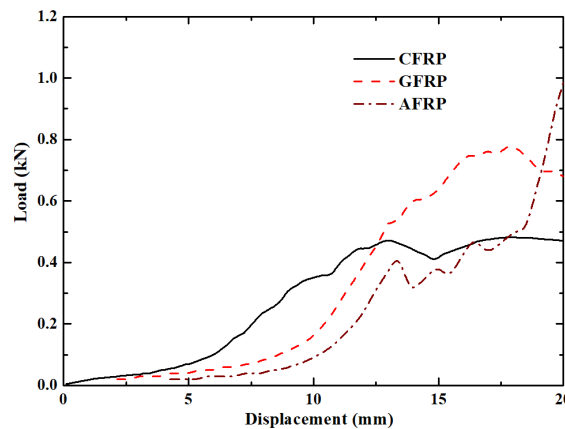


Figure 5. Comparison analysis on load versus displacement traces with three types of composite materials

Figure 6 shows the effect of three types of composite materials on compressive stiffness. The compressive stiffness of GFRP specimens is higher than CFRP and AFRP specimens, with an average value of 42.74 kN/mm. The compressive stiffness of AFRP specimens obtained the lowest average value of 30.43 kN/mm. It was found that specimens with carbon fibre reinforced plastic material had the highest stress requirement in the elastic deformation stage. However, the specimen

with aramid fibre reinforced plastic material shows the lowest stress. It is obtained a slight increasing trend in load versus displacement curves with three types of composite materials. As the load increases, the novel core cell continues to compress and collapse, which results in the densification stage.

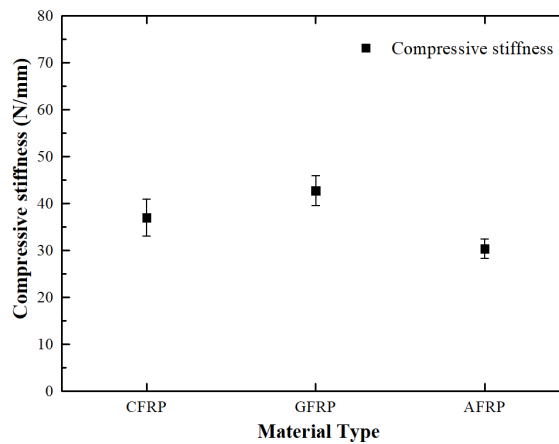


Figure 6. Effect of three types of composite materials on compressive stiffness.

Figure 7 presents the effect of material type on the first peak load of the single spherical-roof contoured-core cell. The minimum average value of peak load is 0.42 kN for AFRP specimen, whereas, the maximum average is 0.78 kN for GFRP specimen. Figure 8 shows the effect of material type on energy absorption (*EA*) and specific energy absorption (*SEA*) parameters. It was found that AFRP specimen obtained the highest specific energy absorption value with 0.69 kJ, and CFRP specimen was the lowest value with 1.44 kJ. Interestingly, it was observed that the GFRP specimen displayed the highest energy absorption value with 2.71 kJ. The SEA of the current spherical-roof contoured-core cell was compared with bonded aluminium egg-box and the best energy-absorbing systems from the references [40, 41]. It was observed that the spherical-roof panels provided the better energy-absorbing capacity, which was around two times greater than the corresponding aluminium egg-box panels.

Images of three types of composite materials on the single spherical-roof contoured-core cell are shown in Figure 9, which are based on compression displacement subjected to the quasi-static loading. During the compression test, the compression platens contacted with the spherical-roof dome and started to crush the specimens. Matrix cracks occurred around the spherical-roof dome, which was as a result of the stress concentration [42]. It was observed that, four supporting points with a curved region were curled up as the loading increased. Moreover, specimens with three types of composite materials showed the same crushing failure behaviour, and the collapse specimen reached the flattened condition, which is in agreement with similar research findings [15, 16, 36].

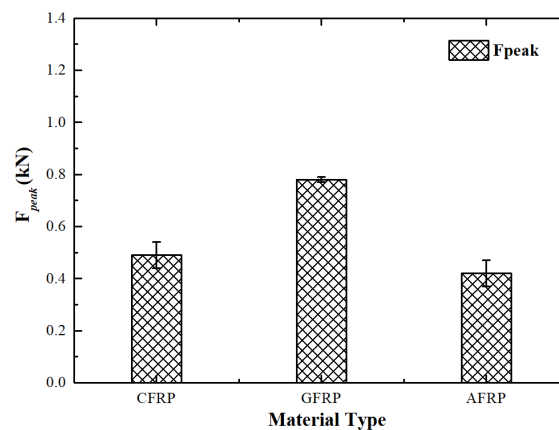


Figure 7. Effect of composite materials on F_{peak} .

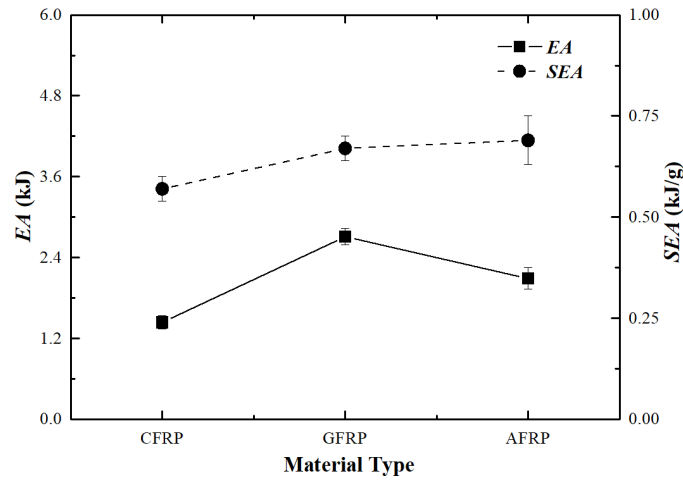


Figure 8. Effect three types of materials on EA and SEA.

Specimens	Compression displacement (mm)			
	5	10	15	20
CFRP				
GFRP				
AFRP				

Figure 9. Photographs of single SRCC cell under quasi-static loading.

The top view images of specimens before and after the test for the three types of composite materials are compared in Figure 10. It could be observed that spherical-roof apex has been flattened inside. This mainly caused by the matrix cracks, fibre fracture and laminates bending according to its structural design. It was concluded that matrix cracks, fibre fracture and laminates bending were typical failure modes of the single contoured-core cell under quasi-static loading. It was proven that the crushing failure behaviour of specimens had no essential relationship with material type. It was observed that matrix cracks occurred around the spherical-roof dome region. Meanwhile, the curved region around the four bottom support points, which showed the typical failure behaviour with unbonded core condition [15, 16, 36].

Specimens	Quasi-static loading	
	Before test	After test
CFRP		
GFRP		
AFRP		

Figure 10. Images of single SRCC cell before and after the quasi-static loading.

The crushing failure behaviour mapping schematics were drawn to understand the failure region and its features, as shown in Figure 11. It was found that failure mapping mainly occurred at the spherical-roof dome region and the curved region. In order to analyse the failure region accurately and specifically, two kinds of zone regions on top view are proposed. The failure region of the spherical-roof dome was measured to obtain its area. Here, zone 1 region is square shape and drawn using yellow colour, which has two diagonals of 8 mm. Zone 2 region is coloured with blue, which showed the same shape and size according to its structural design. It was found that failure cracks mainly occurred around the spherical-roof apex, which is in zone 1 region. Curling edges were folded and damaged by cracks propagated, which followed the zone 2 region boundary. It is highlighted that the damaged mapping schematic diagrams of the spherical-roof contoured-core cell are obtained as in Figure 11. It was concluded that crushing failure has mainly occurred at zone 1 region and zone 2 region boundaries.

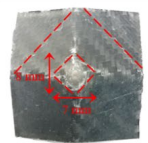
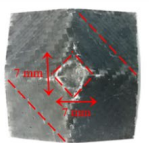
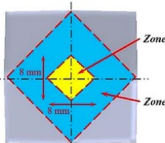
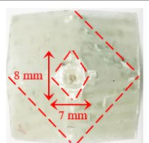
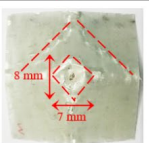
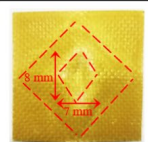
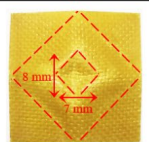
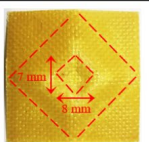
Specimens	Damaged position mapping			Damaged schematic diagram
	1st	2nd	3rd	
CFRP				
GFRP				
AFRP				

Figure 11. Damaged mapping schematic diagrams of single SRCC cell.

CONCLUSION

The energy-absorbing characteristics of the single spherical-roof contoured-core (SRCC) cell were carried out under the quasi-static loading. The crushing behaviour, failure modes, load versus displacement curves were explored through quasi-static loading. Within the limitation of this study, the following conclusions can be drawn:

- i. It was obtained that the compressive stiffness of GFRP specimens is higher than CFRP and AFRP specimens, with an average value of 42.74 kN/mm.
- ii. The three types of composites materials showed the same damage failure behaviour, which are matrix cracks and laminate bending.
- iii. In order to analyse the failure behaviour characteristic and regions of spherical-roof contoured-core cells, zone region concept was proposed. It was highlighted that the crushing failure of this core structure mainly occurred in zone 1 region and around zone 2 region boundaries.

ACKNOWLEDGEMENT

The authors are grateful to the Ministry of Education Malaysia: FRGS/1/2019/TK03/UMP/02/10 and Universiti Malaysia Pahang: RDU180397 for funding this research. This research work is strongly supported by the *Structural Performance Materials Engineering (SUPREME) Focus Group* and the *Human Engineering (HEG) Focus Group*, which provided the research materials and equipment.

REFERENCES

- [1] Sairajan K, Aglietti G, Mani K. A review of multifunctional structure technology for aerospace applications. *Acta Astronautica* 2016;120:30-42.
- [2] Khan M, Syed A, Ijaz H, Shah R. Experimental and numerical analysis of flexural and impact behaviour of glass/PP sandwich panel for automotive structural applications. *Advanced Composite Materials* 2018;27:367-86.
- [3] Wang T, Wang P, Wang Y, Qiao L. A broadband far-field microwave absorber with a sandwich structure. *Materials & Design* 2016;95:486-9.

- [4] Quanjin M, Rejab M, Sahat I, Amiruddin M, Bachtiar D, Siregar J, et al. Design of portable 3-axis filament winding machine with inexpensive control system. *Journal of Mechanical Engineering and Sciences* 2018;12:3479-93.
- [5] Quanjin Ma, Ge J, Rejab M, Sun B, Ding Y, Nie X, et al. Fabrication of the carbon fiber reinforced plastic (CFRP) cone tube through the laboratory-scale 3-axis winding machine. *Materials Today: Proceedings*. Epub ahead of print 14 August 2020. doi.org/10.1016/j.matpr.2020.07.259.
- [6] Quanjin M, Salim M, Rejab M, Bernhardt O-E, Nasution AY. Quasi-static crushing response of square hybrid carbon/aramid tube for automotive crash box application. *Materials Today: Proceedings* 2020;27:683-90.
- [7] Zaid N, Rejab M, Mohamed N. Sandwich Structure Based On Corrugated-Core: A Review. In: *MATEC Web of Conferences*: pp. 00029; 2016.
- [8] Heimbs S, Cichosz J, Klaus M, Kilchert S, Johnson A. Sandwich structures with textile-reinforced composite foldcores under impact loads. *Composite Structures* 2010;92:1485-97.
- [9] Hazizan MA, Cantwell W. The low velocity impact response of foam-based sandwich structures. *Composites Part B: Engineering* 2002;33:193-204.
- [10] Boonkong T, Shen Y, Guan Z, Cantwell W. The low velocity impact response of curvilinear-core sandwich structures. *International Journal of Impact Engineering* 2016;93:28-38.
- [11] Chen Y, Hou S, Fu K, Han X, Ye L. Low-velocity impact response of composite sandwich structures: Modelling and experiment. *Composite Structures* 2017;168:322-34.
- [12] Sun Z, Shi S, Guo X, Hu X, Chen H. On compressive properties of composite sandwich structures with grid reinforced honeycomb core. *Composites Part B: Engineering* 2016;94:245-52.
- [13] Wu Y, Liu Q, Fu J, Li Q, Hui D. Dynamic crash responses of bio-inspired aluminum honeycomb sandwich structures with CFRP panels. *Composites Part B: Engineering* 2017;121:122-33.
- [14] Li S, Li X, Wang Z, Wu G, Lu G, Zhao L. Sandwich panels with layered graded aluminum honeycomb cores under blast loading. *Composite Structures* 2017;173:242-54.
- [15] Haldar A, Zhou J, Guan Z. Energy absorbing characteristics of the composite contoured-core sandwich panels. *Materials Today Communications* 2016;8:156-64.
- [16] Haldar A, Guan Z, Cantwell W, Wang Q. The compressive properties of sandwich structures based on an egg-box core design. *Composites Part B: Engineering* 2018;144:143-52.
- [17] Cai Z-Y, Zhang X, Liang X-B. Multi-point forming of sandwich panels with egg-box-like cores and failure behaviors in forming process: Analytical models, numerical and experimental investigations. *Materials & Design* 2018;160:1029-41.
- [18] Zaid N, Rejab M, Jusoh A, Bachtiar D, Siregar J. Effect of varying geometrical parameters of trapezoidal corrugated-core sandwich structure. In: *MATEC Web of Conferences*: pp. 01018; 2017.
- [19] Rejab M, Ruzaimi M, Zaid N, Siregar JP, Bachtiar D. Scaling effects for compression loaded of corrugated-core sandwich panels. *Advanced Materials Research* 2016;1133:241-245.
- [20] Yahaya MA, Ruan D, Lu G, Dargusch M. Response of aluminium honeycomb sandwich panels subjected to foam projectile impact—An experimental study. *International Journal of Impact Engineering* 2015;75:100-9.
- [21] Liu C, Zhang Y, Li J. Impact responses of sandwich panels with fibre metal laminate skins and aluminium foam core. *Composite Structures* 2017;182:183-90.
- [22] Wu Q, Gao Y, Wei X, Mousanezhad D, Ma L, Vaziri A, et al. Mechanical properties and failure mechanisms of sandwich panels with ultra-lightweight three-dimensional hierarchical lattice cores. *International Journal of Solids and Structures* 2018;132:171-87.
- [23] Norouzi H, Rostamiyan Y. Experimental and numerical study of flatwise compression behavior of carbon fiber composite sandwich panels with new lattice cores. *Construction and Building Materials* 2015;100:22-30.
- [24] Rejab M, Cantwell W. The mechanical behaviour of corrugated-core sandwich panels. *Composites Part B: Engineering* 2013;47:267-77.
- [25] Qu J, Ju D, Gao S, Chen J. Research on the dynamic mechanical properties of polymethacrylimide foam sandwich structure. *Composite Structures* 2018;204:22-30.
- [26] Dong L, Wadley H. Shear response of carbon fiber composite octet-truss lattice structures. *Composites Part A: Applied Science and Manufacturing* 2016;81:182-92.
- [27] George T, Deshpande VS, Wadley HN. Mechanical response of carbon fiber composite sandwich panels with pyramidal truss cores. *Composites Part A: Applied Science and Manufacturing* 2013;47:31-40.
- [28] Chen M, Zhu X, Lei H, Chen H, Fang D. Effect of defect on the compressive response of sandwich structures with carbon fiber pyramidal truss cores. *International Journal of Applied Mechanics* 2015;7:1550004.
- [29] Xiong J, Ma L, Wu L, Wang B, Vaziri A. Fabrication and crushing behavior of low density carbon fiber composite pyramidal truss structures. *Composite Structures* 2010;92:2695-702.
- [30] Jiang S, Sun F, Zhang X, Fan H. Interlocking orthogrid: an efficient way to construct lightweight lattice-core sandwich composite structure. *Composite Structures* 2017;176:55-71.
- [31] Jin M, Hu Y, Wang B. Compressive and bending behaviours of wood-based two-dimensional lattice truss core sandwich structures. *Composite Structures* 2015;124:337-44.

- [32] Lin D, Ni R, Adams R. Prediction and measurement of the vibrational damping parameters of carbon and glass fibre-reinforced plastics plates. *Journal of Composite Materials* 1984;18:132-52.
- [33] Zinno A, Fusco E, Prota A, Manfredi G. Multiscale approach for the design of composite sandwich structures for train application. *Composite Structures* 2010;92:2208-19.
- [34] Borsellino C, Calabrese L, Valenza A. Experimental and numerical evaluation of sandwich composite structures. *Composites Science and Technology* 2004;64:1709-15.
- [35] Haldar A, Managuli V, Munshi R, Agarwal R, Guan Z. Compressive Behaviour of 3D Printed Sandwich Structures Based on Corrugated Core Design. *Materials Today Communications* 2020:101725.
- [36] Quanjin M, Rejab M, Idris M, Merzuki M, Shaoliang H. Compressive properties on the spherical-roof contoured-core cell with different amounts of diamond-shaped notches. In: *IOP Conference Series: Materials Science and Engineering*: pp. 012049; 2020.
- [37] Karlsson KF, TomasÅström B. Manufacturing and applications of structural sandwich components. *Composites Part A: Applied Science and Manufacturing* 1997;28:97-111.
- [38] Lyu M-Y, Choi TG. Research trends in polymer materials for use in lightweight vehicles. *International Journal of Precision Engineering and Manufacturing* 2015;16:213-20.
- [39] Feng NL, DharMalingam S, Zakaria KA, Selamat MZ. Investigation on the fatigue life characteristic of kenaf/glass woven-ply reinforced metal sandwich materials. *Journal of Sandwich Structures & Materials* 2017:1099636217729910.
- [40] Zupan M, Chen C, Fleck N. The plastic collapse and energy absorption capacity of egg-box panels. *International Journal of Mechanical Sciences* 2003;45:851-71.
- [41] Yoo S, Chang S, Sutcliffe M. Compressive characteristics of foam-filled composite egg-box sandwich panels as energy absorbing structures. *Composites Part A: Applied Science and Manufacturing* 2010;41:427-34.
- [42] Chung J, Chang S, Sutcliffe M. Deformation and energy absorption of composite egg-box panels. *Composites Science and Technology* 2007;67:2342-9.